Carbon-13 Nuclear Magnetic Relaxation in Macromolecules with Side Chains Undergoing Multiple Internal Rotations. Effects of the Distribution of Correlation Times and Overall Anisotropic Motion

Akihiro Tsutsumi* and Claude Chachaty

Service de Chimie Physique, Centre d'Etudes Nucléaires de Saclay, 91190, Gif-sur-Yvette, France. *Received December 4, 1978*

ABSTRACT: Dipolar nuclear magnetic relaxation in macromolecules having side chains which undergo multiple internal rotations has been investigated for two cases: (1) the motion of the molecule as a whole is anisotropic and (2) there is a distribution of correlation times in the main chain. It is assumed that the internal rotations of the side chain occur by random jumps among sites 1, 2, and 3, two of which are equivalent. The rates of internal rotations are specified by three jump rates, W_1 ($1 \rightarrow 2$ or $1 \rightarrow 3$), W_2 ($2 \rightarrow 1$ or $3 \rightarrow 1$), and W_3 ($2 \rightleftarrows 3$). The theoretical equations for spin-lattice relaxation times (T_1), spin-spin relaxation times (T_2), and Nuclear Overhauser Enhancements (NOE) of ^{13}C {^{1}H} are given. Some numerical calculations of T_1 and NOE are presented for two typical conditions of internal rotations of an alkyl side chain: (1) $W_1 = \upsilon W_2$, $W_3 = 0$ and (2) $W_1 = \upsilon W_2$, $W_3 = W_2$. The effects of an overall anisotropic motion of the macromolecule and of the distribution of correlation times in the main chain on the ^{13}C relaxation of the side chain are discussed. The frequency dependence of this latter is also examined.

With the recent advances in Fourier transform NMR spectroscopy it becomes possible to determine the ^{1}H and ^{13}C relaxation times in molecules of increasing complexity. The interpretation of the relaxation data in terms of molecular dynamics requires a thorough knowledge of the effects of overall and internal motions which have been subjected to many investigations in the last few years.[1-16] The basic theory for the effects of internal rotation on nuclear relaxation has been provided first by Woessner,[17] and then extended to molecules undergoing multiple internal motions.[6,18,19]

The two models of Woessner are the rotational jump among three equivalent sites and the unrestricted rotational diffusion.[17] However, it happens generally that the different rotamers about a given bond are not equally populated and that the diffusion is limited to a restricted angular range. Such problems have been treated by London and Avitabile,[5] Tsutsumi,[20] and Gronski and Murayama.[21] London and Avitabile[5] and Tsutsumi[20] have proposed the model of jumps among three sites, two of which are equivalent. The former treatment, however, is applicable only to saturated hydrocarbon chains. On the other hand, the latter can also be applied to chains containing groups other than saturated hydrocarbons.

Further important problems of the anisotropy of the overall motion and of the distribution of correlation times have been investigated by Levine et al.[22] and Levy et al.[4] for the case of an unrestricted rotational diffusion only. However, for aliphatic chains, a more realistic model is the rotational jump among three sites corresponding to the trans (t) and gauche (g^+, g^-) conformers. In connection with this, Witterbort and Szabo[23] have treated the relaxation in side chains attached to a symmetrical rotor, using the model of jumps among the allowed conformations on a tetrahedral lattice. This model is a noticeable improvement over previous treatments, where all internal rotations are assumed to be independent or uncoupled from each other, although such an attempt has already been made by use of the Monte-Carlo method.[13-15,24]

In this work, we have extended our previous model of internal rotations,[20] which has been used for a molecule with one internal bond, to systems with multiple internal rotations as in macromolecules having side chains and examined the effects of the anisotropic motion and of the distribution of correlation times of the main chain on the side chain relaxation. Although our treatment is limited within the framework of independent internal rotations, it develops the previous treatments in this field and is considered to have further potentialities for investigating the dynamics of chain molecules.

The jump model used here is not limited to three sites separated by an angle of 120°, this angle being changeable. The model can be modified easily for jumps between two equivalent sites separated by a variable angle,[10] which includes the treatment of Jones,[25] or between two nonequivalent sites separated by an angle of 180°. Furthermore, our treatment may be readily extended to the case of side chains including rigid groups such as allyl, phenyl, and peptide. The numerical calculations for this treatment are given for the example of the ^{13}C dipolar relaxation in normal alkyl side chains of a macromolecule where rotational jump occurs among t, g^+, g^- conformers about C–C bonds. Some applications to poly(amino acids) and poly(alkylvinylpyridine) will be published in the near future.

Theory

The nuclear spin relaxation times T_1 and T_2 and Nuclear Overhauser Enhancement NOE for ^{13}C {^{1}H} are given by:[26]

$$T_1^{-1} = {}^1\!/_{20}K[J_0(\omega_C - \omega_H) + 3J_1(\omega_C) + 6J_2(\omega_C + \omega_H)] \qquad (1)$$

$$T_2^{-1} = {}^1\!/_{40}K[4J_0(0) + J_0(\omega_C - \omega_H) + 3J_1(\omega_C) + 6J_1(\omega_H) + 6J_2(\omega_C + \omega_H)] \qquad (2)$$

$$\mathrm{NOE} = 1 - \frac{\gamma_H}{\gamma_C}\,\frac{J_0(\omega_C - \omega_H) - 6J_2(\omega_C + \omega_H)}{J_0(\omega_C - \omega_H) + 3J_1(\omega_C) + 6J_2(\omega_C + \omega_H)} \qquad (3)$$

with $K = \gamma_C^2\gamma_H^2\hbar^2r^{-6}$, where γ_C and γ_H and ω_C and ω_H are the nuclear gyromagnetic ratios and the angular resonance frequencies for ^{13}C and ^{1}H nuclei, respectively. r is the time-independent ^{13}C–^{1}H distance. The $J_h(\omega)$ are the Fourier transform of the angular autocorrelation function defined by

$$J_h(\omega) = \int_{-\infty}^{\infty} G_h(\tau)e^{i\omega\tau}\,d\tau \qquad (4)$$

$$G_h(\tau) = \langle F(t)F^*(t + \tau)\rangle \qquad (5)$$

---

* Address correspondence to this author at the Department of Polymer Science, Faculty of Science, Hokkaido University, Sapporo 060, Japan.

0024-9297/79/2212-0429$01.00/0

where $F(t)$ is the angular part of the dipolar interaction function. $F_h(t)$ can be expressed in terms of the second order Wigner rotation matrices $D^{(2)}_{mn}(t)$.[27] θ and φ are the polar and the azimuthal angles of the spin pair vector, respectively; in the laboratory coordinate system with the z axis along the magnetic field, $F_h(t)$ can be written as

$$F_0(t) = D^{(2)}_{00}(t) = \tfrac{1}{2}(3\cos^2\theta - 1) \qquad (6.1)$$

$$F_{\pm1}(t) = D^{(2)}_{\pm10}(t) = \mp(\tfrac{3}{2})^{1/2}(\sin\theta\cos\theta)e^{\mp i\varphi} \qquad (6.2)$$

$$F_{\pm2}(t) = D^{(2)}_{\pm20}(t) = (\tfrac{3}{8})^{1/2}(\sin^2\theta)e^{\mp2i\varphi} \qquad (6.3)$$

The autocorrelation function for a long chain connected to a rigid anisotropic rotor can be easily formulated by similar procedures reported previously,[6,18,19,22] where the internal and overall motions are assumed to be completely independent. The autocorrelation function for the Nth ^{13}C–^{1}H pair becomes

$$G_h(\tau) = \tfrac{1}{5} \sum_{\substack{smrab...n\\a'b'...n'}} [e^{-E_s\tau}T_m(s)T_r(s)e^{-i\alpha_0(m-r)}d^{(2)}_{ma}(\beta_0)d^{(2)}_{ra'}(\beta_0)d^{(2)}_{ab}(\beta_1) \times d^{(2)}_{a'b'}(\beta_1)...d^{(2)}_{no}(\beta_N)d^{(2)}_{n'o}(\beta_N)e^{-i\alpha_N(n-n')}\langle e^{-i\{a\gamma_1(0)-a'\gamma_1(\tau)\}}\rangle ... \langle e^{-i\{n\gamma_N(0)-n'\gamma_N(\tau)\}}\rangle] \qquad (7)$$

where $T_m(s)$, which corresponds to $a^{(2)}_m(s)$ in ref 19, is the coefficient of the eigenfunction for the diffusion equation of the anisotropic rotor, and E_s is the corresponding eigenvalue.[19] β_0 and α_0 are the polar and azimuthal angles of the first bond, respectively, with respect to the coordinate fixed to the rotor. $\beta_1...\beta_{N-1}$ are the angles between neighboring bonds along the chain (for saturated carbon chain these angles are the complement of the tetrahedral angle, i.e., 70.5°). β_N and α_N are the polar and azimuthal angles of the Nth carbon–hydrogen bond C_N–H, respectively, with respect to the coordinate fixed in the Nth group, where the z axis is parallel to the C_{N-1}–C_N bond, and the x axis is in the plane defined by C_{N-1}, C_N, and C_{N+1} and perpendicular to the C_{N-1}–C_N bond. For the methylene group, $\alpha_N = +120°$ and $\beta_N = 70.5°$. $d^{(2)}_{mn}(\beta)$ is the reduced second-order Wigner rotation matrix.[27] $\gamma_N(t)$ is the dihedral angle defined by the carbons C_{N-2}, C_{N-1}, C_N, and C_{N+1}. All indices run from −2 to 2. The angular brackets represent the ensemble average, which depends on the various configurations and motions of the individual internal bond. It is postulated here that each bond can jump among three sites as shown below for the Nth bond.[20]

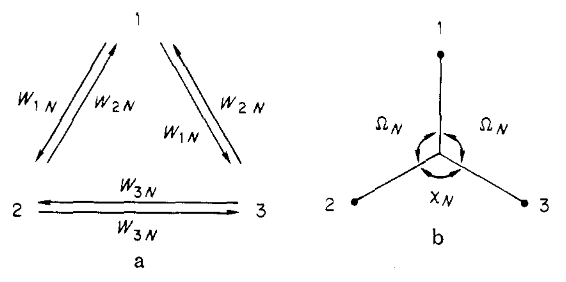

In these schemes, sites 1, 2, and 3 represent the possible position of the C_{N+1} carbon with respect to C_{N-2} in the Newman projection of the C_{N-2}, C_{N-1}, C_N, and C_{N+1} fragment. In our calculation, the position of site 1 is specified by the angle ϵ_N. Ω_N and χ_N are the angular separations between the sites. W_{iN} is a jump rate between two sites. The specification of the jump rates as in (a) leads to sites 2 and 3 being equivalent. In the aliphatic chains where $\epsilon_N = 180°$ and $\Omega_N = 120°$, the sites 1, 2, and 3 correspond to the t, g^+, and g^- conformers about the C_{N-1}–C_N bond. The condition $\chi_N = 0°$ leads to jumps between two nonequivalent sites separated by 180°. The jumps between two equivalent sites separated by an angle χ_N[10] correspond to $W_{1N}/W_{2N} \gg 1$.

The rate equation for the Nth bond becomes:

$$\frac{d\mathbf{P}_N(t)}{dt} = \mathbf{W}_N\mathbf{P}_N(t) \qquad (8)$$

where $\mathbf{P}_N(t)$ is a time-dependent occupational probability, the components $P_{1N}(t)$, $P_{2N}(t)$, and $P_{3N}(t)$ of which correspond to sites 1, 2, and 3, respectively. $\mathbf{W}_N$ is the matrix of kinetic coefficients:

$$\mathrm{W}_N = \begin{bmatrix} -2W_{1N} & W_{2N} & W_{2N} \\ W_{1N} & -(W_{2N} + W_{3N}) & W_{3N} \\ W_{1N} & W_{3N} & -(W_{2N} + W_{3N}) \end{bmatrix} \qquad (9)$$

Diagonalization of $\mathbf{W}_N$ leads to

$$\Lambda_N \quad \begin{bmatrix} \lambda_{1N} & & \\ & \lambda_{2N} & \\ & & \lambda_{3N} \end{bmatrix} \qquad (10)$$

where $\lambda_{1N} = 0$, $\lambda_{2N} = 2W_{1N} + W_{2N}$, and $\lambda_{3N} = W_{2N} + 2W_{3N}$.

The conditional probability $R_{ijN}(t)$, which is the probability in site i at $t = 0$ to be found in site j at time t, can be obtained by solving eq 8 under the conditions $\mathbf{R}_N(0) = 1$ and $\sum_i R_{ijN}(t) = 1$, eq 11, where $\upsilon_N = W_{1N}/W_{2N}$, $a_N = 2\upsilon_N + 1$, $B_N(2) = e^{-\lambda_{2N}t}$, and $B_N(3) = e^{-\lambda_{3N}t}$. We define $B_N(1) = e^{-\lambda_{1N}t}$.

$$\mathrm{R}_N(t) = \begin{bmatrix} 1 + 2\upsilon_N B_N(2) & 1 - B_N(2) & 1 - B_N(2) \\ \upsilon_N - \upsilon_N B_N(2) & \upsilon_N + \tfrac{1}{2}B_N(2) + \tfrac{1}{2}a_N B_N(3) & \upsilon_N + \tfrac{1}{2}B_N(2) - \tfrac{1}{2}a_N B_N(3) \\ \upsilon_N - \upsilon_N B_N(2) & \upsilon_N + \tfrac{1}{2}B_N(2) - \tfrac{1}{2}a_N B_N(3) & \upsilon_N + \tfrac{1}{2}B_N(2) + \tfrac{1}{2}a_N B_N(3) \end{bmatrix} \qquad (11)$$

The equilibrium occupational probabilities are

$$P_{iN}(\infty) = R_{ijN}(\infty) \qquad (12)$$

The ensemble average can be evaluated from

$$\langle e^{-i\{n\gamma_N(0)-n'\gamma_N(\tau)\}}\rangle = \sum_{i,j=1}^{3} P_{iN}(\infty)R_{ijN}(\tau)e^{-i\{n\gamma_{iN}-n'\gamma_{jN}\}} \qquad (13)$$

where $\gamma_{1N} = \epsilon_N$, $\gamma_{2N} = \epsilon_N + \Omega_N$, and $\gamma_{3N} = \epsilon_N - \Omega_N$.

The complete expression becomes:

$$\langle e^{-i\{n\gamma_N(0)-n'\gamma_N(\tau)\}}\rangle = \sum_{q_N=1}^{3} A_{Nnn'}(q_N)B_N(q_N) \qquad (14)$$

where

$$A_{Nnn'}(1) = a_N^{-2}\{1 + 2\upsilon_N\cos(n\Omega_N)\}\{1 + 2\upsilon_N\cos(n'\Omega_N)\}e^{-i(n-n')\epsilon_N} \qquad (15.1)$$

$$A_{Nnn'}(2) = 2\upsilon_N a_N^{-2}\{1 - \cos(n\Omega_N)\}\{1 - \cos(n'\Omega_N)\}e^{-i(n-n')\epsilon_N} \qquad (15.2)$$

$$A_{Nnn'}(3) = 2\upsilon_N a_N^{-1}\sin(n\Omega_N)\sin(n'\Omega_N)e^{-i(n-n')\epsilon_N} \qquad (15.3)$$

In eq 14, $q_N = 1, 2, 3$ correspond to the motion about the Nth bond with different rate constants.

We can obtain the autocorrelation function $G_h(\tau)$ by substitution of eq 14 into eq 7. We assume here that the anisotropic motion is axially symmetric with the diffusion coefficients $D_\parallel$ and $D_\perp$. In this case, the Fourier transform of $G_h(\tau)$ becomes:

$$J_h(\omega) = \tfrac{2}{5} \sum_{\substack{mab...n,q_1...q_N\\a'b'...n'}} [d^{(2)}_{ma}(\beta_0)d^{(2)}_{ma'}(\beta_0)d^{(2)}_{ab}(\beta_1)d^{(2)}_{a'b'}(\beta_1)...d^{(2)}_{no}(\beta_N) \times d^{(2)}_{n'o}(\beta_N)e^{-i(n-n')\alpha_N}A_{1aa'}(q_1)...A_{Nnn'}(q_N)f(\tau^*)] \qquad (16)$$

where

$$f(\tau^*) = \frac{\tau^*}{1 + \omega^2\tau^{*2}} \qquad (17)$$

$$\tau^* = \{6D_\perp + m^2(D_\parallel - D_\perp) + \sum_{k=1}^{N}\lambda_{q_k,k}\}^{-1} \qquad (18)$$

In the case of isotropic overall motion, we have the relation $D_\parallel = D_\perp = D$, where D is the isotropic diffusion coefficient and is related to the isotropic correlation time τ_R by $D = {}^1/{}_6\tau_R$. Using the orthonormality condition[27]

$$\sum_m d_{ma}^{(2)}(\beta_0)d_{ma'}^{(2)}(\beta_0) = \delta_{aa'} \qquad (19)$$

we can write $J_h(\omega)$ as

$$J_h(\omega) = {}^2/{}_5 \sum_{\substack{ab...n,q_1...q_N \\ b'...n'}} [d_{ab}^{(2)}(\beta_1)d_{a'b'}^{(2)}(\beta_1)...d_{no}^{(2)}(\beta_N)d_{n'o}^{(2)}(\beta_N)e^{-i(n-n')\alpha_N} \times A_{1aa'}(q_1)...A_{Nnn'}(q_N)f(\tau_p)] \qquad (20)$$

where

$$\tau_p = \{\tau_R^{-1} + \sum_{k=1}^{N}\lambda_{q_k,k}\}^{-1} \qquad (21)$$

When there is a distribution for τ_R, $f(\tau_p)$ must be averaged over a range of the distribution. In our calculations, we have chosen the Cole–Cole distribution[28] of correlation times, the density function of which is:[29]

$$F(s) = \frac{1}{2\pi}\frac{\sin(\gamma\pi)}{\cosh(\gamma s) + \cos(\gamma\pi)} \qquad (22)$$

s being

$$s = \ln(\tau_R/\tau_A) \qquad (23)$$

where τ_A is the average correlation time. γ is the distribution width parameter ($0 < \gamma \leq 1$). $\gamma = 1$ corresponds to the single distribution. In the case of no internal rotation, the second term in eq 21 is zero, and the averaging of $f(\tau_p)$ becomes[29]

$$\overline{f(\tau_p)} = \frac{1}{2\omega}\frac{\cos[(1-\gamma)\pi/2]}{\cosh(\gamma\ln\omega\tau_A) + \sin[(1-\gamma)\pi/2]} \qquad (24)$$

When there is internal rotation, the averaging has to be evaluated numerically.

Results and Discussion

To illustrate the influence of the different parameters involved in the calculations of the ^{13}C longitudinal relaxation time, we have selected two typical cases denoted hereafter as cases (1) and (2) for a saturated hydrocarbon chain undergoing rotational jumps among t, g^+, and g^- local forms, taking therefore $\Omega = 120°$ and $\epsilon = 180°$: $W_1(t \rightarrow g^\pm) = vW_2(g^\pm \rightarrow t)$ with $W_3(g^\pm \rightleftarrows g^\mp) = 0$ (case (1)) or $W_3 = W_2$ (case (2)). In actual cases, there may be a variety of jump rates around the carbon–carbon bond, depending upon the chain length and molecular structures. Particularly for side chains having a large pendant group, the jump rates will be somewhat different from the values expected for a normal aliphatic chain. In our numerical calculations, however, we are mainly concerned with the effects of the anisotropic motion and of the distribution of correlation times on the relaxation of side chain carbons, and we have assumed for simplicity that the jump rates $W_{1,2,3}$ are independent of the carbon positions.

1. Effects of Anisotropic Motion of Main Chain on the Relaxation of Side Chain Carbons. Figure 1 shows the dependence of T_1 on the ratio $D_\parallel/D_\perp$ which is a measure of the anisotropic motion. W_2, hereafter we take off the suffix indicating carbon position, and v are fixed to 10^{10} s^{-1} and 0.5, respectively, for both case (1) and case (2). For $D_\parallel = 10^{10}$ s^{-1} where $(\omega_c + \omega_H)/6D_\parallel \ll 1$, T_1 is found to decrease rapidly with $D_\perp$ indicating that the relaxation process is governed by the smallest component of the diffusion tensor. This trend is particularly apparent for carbons close to the main chain. Taking $D_\parallel = 10^9$ s^{-1}, i.e., smaller than the jump rates, the dependence of T_1 upon $D_\parallel/D_\perp$ is significantly reduced and the contributions of the internal motions of side chain become predominant with a subsequent reduction of the effect of the overall anisotropic motion. Figure 1 indicates also that T_1 is larger in case (2) than in case (1) as a consequence of the difference in the internal rotational freedom.

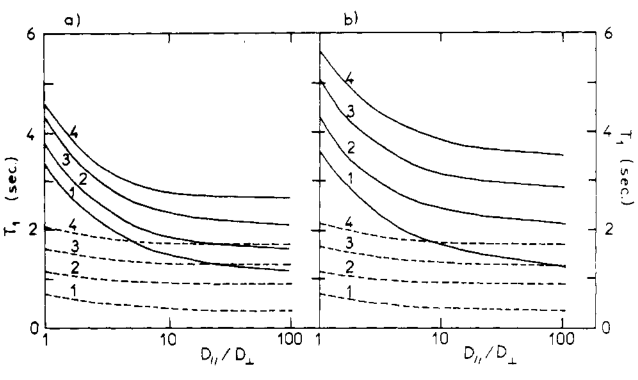

Figure 1. Dependence of T_1 on the ratio $D_\parallel/D_\perp$ at the resonance frequency 25.2 MHz. The full and dotted curves correspond to $D_\parallel = 10^{10}$ s^{-1} and $D_\parallel = 10^9$ s^{-1}, respectively. W_1 and W_2 are fixed to 5×10^9 s^{-1} and 10^{10} s^{-1}, respectively ($v = 0.5$), $\beta_0 = 45°$: (a) case (1), and (b) case (2). The numbering of the curves refers to the carbons of alkyl side chains, carbon 1 being directly attached to the main chain.

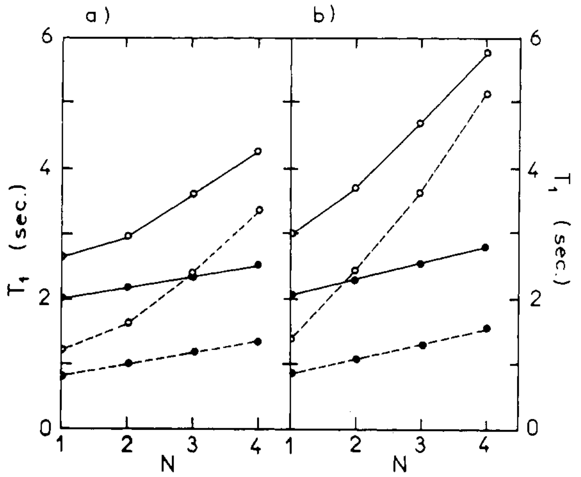

Figure 2. Dependence of T_1 on the carbon number N at the resonance frequency 25.2 MHz. The full and dotted lines correspond to $D_\parallel/D_\perp = 2$ and 100, respectively, with $D_\parallel = 10^{10}$ s^{-1}. W_2 is 10^{10} s^{-1}. The open and closed circles correspond to $v = 1$ and 0.1, respectively, $\beta_0 = 45°$: (a) case (1), and (b) case (2). In this figure and the subsequent ones N is the carbon number.

The dependence of T_1 upon the freedom of internal rotation is also clearly demonstrated in Figure 2, where $v(W_1/W_2)$ was taken as 1 and 0.1 for $D_\parallel/D_\perp = 2$ and 100. T_1 increases with the carbon number, starting from the main chain, but the gradient along the chain is considerably different for the two values of v. A similar effect has been reported by London[5] for a molecule tumbling isotropically with an internal rotation corresponding to case (1). In the present case, however, the dependence of T_1

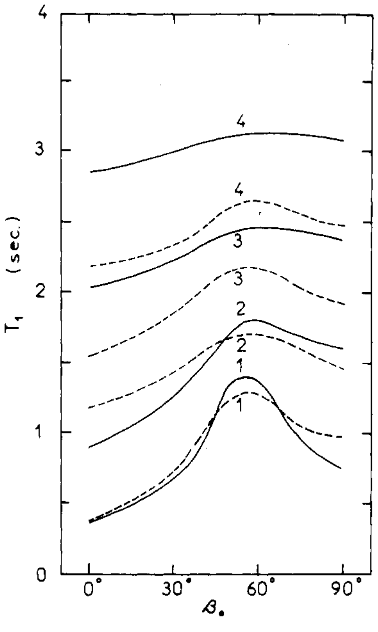

Figure 3. Dependence of T_1 on β_0 at the resonance frequency 25.2 MHz for case (1) with $W_2 = 10^{10}$ s^{-1} and $D_{\|}/D_{\perp} = 100$ ($D_{\|} = 10^{10}$ s^{-1}). The full and dotted curves correspond to $v = 1$ and 0.5, respectively.

upon v is affected by the ratio $D_{\|}/D_{\perp}$, being larger for the smaller value of v. For $v = 0.1$, the pronounced effect is seen over the entire side chain, whereas for $v = 1$, it diminishes as the carbon number increases, particularly in case (2). These results indicate that the effect of the anisotropic motion depends considerably upon the motional freedom of the carbon chain, which may be caused by altering the side chain length or the jump rates themselves.

In the above calculations, the angle β_0 between the first bond, C_0–C_1, and the molecular z axis is fixed to 45°. However, the most characteristic effects of the anisotropic motion can be obtained by varying the angle β_0. For completeness, we will briefly consider this.

Figure 3 shows the effects of altering β_0 for case (1) only. Calculations were made for $D_{\|}/D_{\perp} = 100$ with $D_{\|} = 10^{10}$ s^{-1}, and $v = 0.5$ and 1 with $W_2 = 10^{10}$ s^{-1}. For the first carbon, T_1 increases with β_0 and reaches a maximum value near $\beta_0 = 54°44'$, and then decreases. This phenomenon becomes more pronounced for larger $D_{\|}$ and $D_{\|}/D_{\perp}$ values and has been pointed out by Levine et al.[22] for the unrestricted diffusional rotation model. This point is explained in terms of the contribution of matrix elements $d_{ma}^{(2)}(\beta_0)$ to the relaxation. Detailed explanations are similar to those given by Levine et al.[22] For $v = 1$, such β_0 dependence becomes less marked with the increase of the carbon number than for $v = 0.5$. Particularly for the fourth carbon, the maximum almost disappears, and T_1 increases but slightly with β_0. However, for $v = 0.5$, the shape of the curve does not vary so much with the carbon number, and the maximum is still observed for the fourth carbon. Such a difference can be explained by the dependence of the motional freedom of the side chain upon v, which affects the average orientation of the carbon–hydrogen bond to the molecular z axis.

2. Effects of the Distribution of Correlation Times in Main Chain on the Relaxation of Side Chain Carbons. The effects of the distribution of correlation times on the ^{13}C longitudinal relaxation have been investigated using the Cole–Cole distribution function for an isotropic motion of the main chain. Most of calculations were made for two values of distribution width parameter, $\gamma = 1$ (single distribution) and $\gamma = 0.6$ (the logarithmic width at half-height is 1.61).

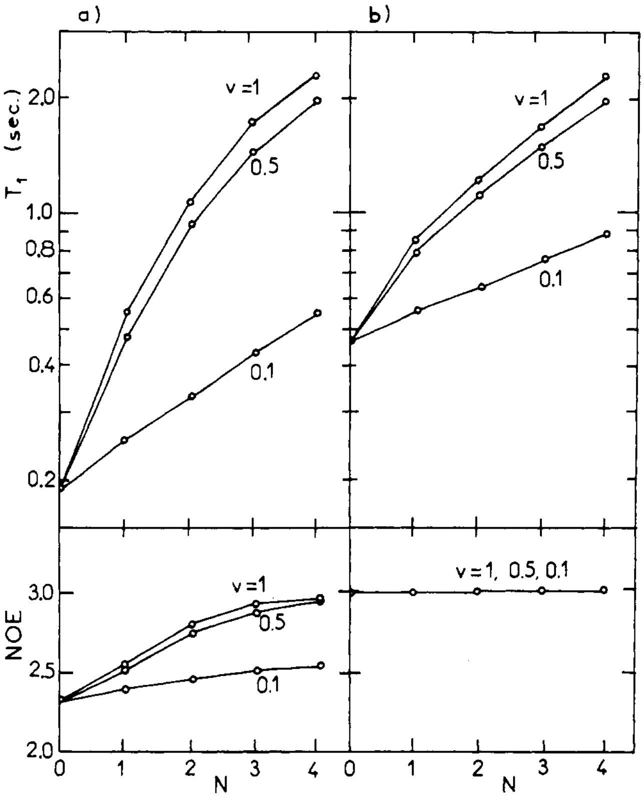

Figure 4. Plot of T_1 and NOE against carbon number N for case (1) with $v = 0.1$, 0.5, and 1 ($W_2 = 10^{10}$ s^{-1}). The resonance frequency is 25.2 MHz, $\tau_A = 10^{-10}$ s: (a) $\gamma = 0.6$, and (b) $\gamma = 1$. $N = 0$ designates a carbon of the main chain.

The diagrams shown in Figure 4 are given for case (1) with $W_2 = 10^{10}$ s^{-1} and $\tau_A = 10^{-10}$ s. This τ_A value corresponds to the left-hand side region of the T_1 vs. τ_A curve for a molecule having no internal rotations, where the condition $\omega\tau_A < 1$ holds. In this region, T_1 is always smaller for $\gamma < 1$ than for $\gamma = 1^8$ except for the region close to the T_1 minimum ($\tau_A = 5 \times 10^{-9}$ s at $\omega(^{13}C) = 1.58 \times 10^8$ rad s^{-1}). In Figure 4, this effect is seen for the zeroth carbon from the main chain. The T_1 gradient along the chain strongly depends on v. This feature is similar to Figure 2, but it is now for the case of an isotropic overall motion. A comparison between the results obtained with $\gamma = 1$ and 0.6 shows that the v dependence increases with the width of the distribution. It is also observed that the T_1 gradient is greatly increased by a broadening of the distribution, which is very important at smaller v. These results indicate that the distribution of correlation times has a large influence on the relaxation in the side chain. The effects are particularly pronounced for the first carbon, where the reorientation of the carbon–hydrogen bond is highly restricted compared with others.

Figure 4 shows that the distribution also has a large influence on the NOE of ^{13}C. For $\gamma = 1$, the dependence of NOE upon v and the carbon number is indeed quite small, becoming very important for $\gamma = 0.6$.

The influence of the parameter γ on the ^{13}C relaxation times, calculated for a jump model for three equivalent sites, is represented on Figure 5. The distribution effect is still significant, although less marked than for three nonequivalent sites (Figure 4) because of a comparatively larger freedom of internal motion.

We have also considered the case where both τ_A and the resonance frequency are varied. Figure 6 shows the plots of T_1 as a function of τ_A for two resonance frequencies, 25.2

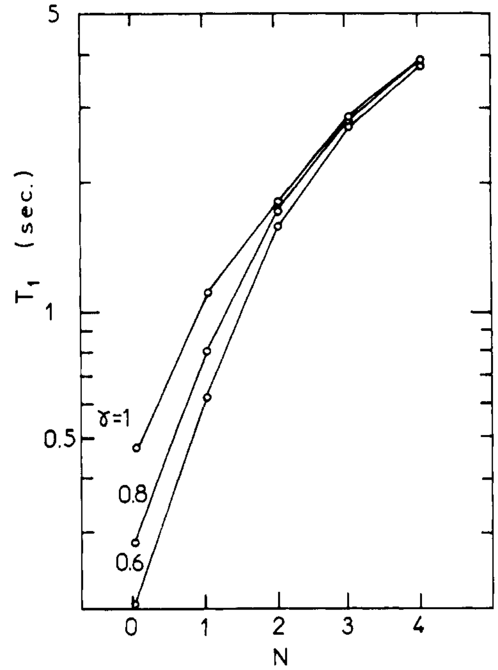

Figure 5. Dependence of T_1 on the carbon number N at the resonance frequency of 25.2 MHz for case (2) with $W_1 = W_2 = W_3 = 10^{10}$ s^{-1} and $\tau_A = 10^{-10}$ s^{-1}. γ = 0, 6, 0.8, and 1.

and 63 MHz. For $\gamma = 1$ (Figure 6b), it is found that the overall motion is an important factor for the relaxation when τ_A is much less than the reciprocal of jump rates. T_1 approaches rapidly a single value for all carbons when τ_A decreases. For $\gamma = 0.6$ (Figure 6a), on the other hand, there is still a pronounced gradient of T_1 along the chain even for very short τ_A (10^{-11} s).

In the region where τ_A is much larger than the reciprocal of the jump rates ($\tau_A > 10^{-7}$ s), the distribution effect of T_1 is not so significant except for the zeroth carbon. In this region, the contribution from internal motion becomes more important in the side chain carbons, since the first term in eq 21 becomes negligibly small compared with the second one.

For the intermediate region which is near the T_1 minimum, we can point out two noticeable points, although the T_1 behavior is somewhat complex; in all carbons the T_1 minimum for $\gamma = 0.6$ is shallower than for $\gamma = 1$, and the correlation time at the T_1 minimum shifts to a larger value with increase of the carbon number, this effect becoming more marked as the distribution broadens.

From the diagrams of Figure 6, we can investigate the influence of the distribution on the estimates of jump rates from experimental T_1. For $\gamma = 1$, T_1 of the zeroth carbon at $\tau_A = 10^{-10}$ s is 0.47 s. On the other hand, for $\gamma = 0.6$, the same T_1 value corresponds to $\tau_A = 1.6 \times 10^{-11}$ s. The T_1 of the side chain carbons for these τ_A values are given in Figure 7. It is found that the T_1 gradient is smaller for $\gamma = 1$ than $\gamma = 0.6$ in spite of using the same jump rates. This feature indicates that if the experimental data were analyzed with a single distribution, one would obtain somewhat larger jump rates than the actual ones, since for a broader distribution the jump rates have to be diminished to obtain the same T_1 values as for the single distribution.

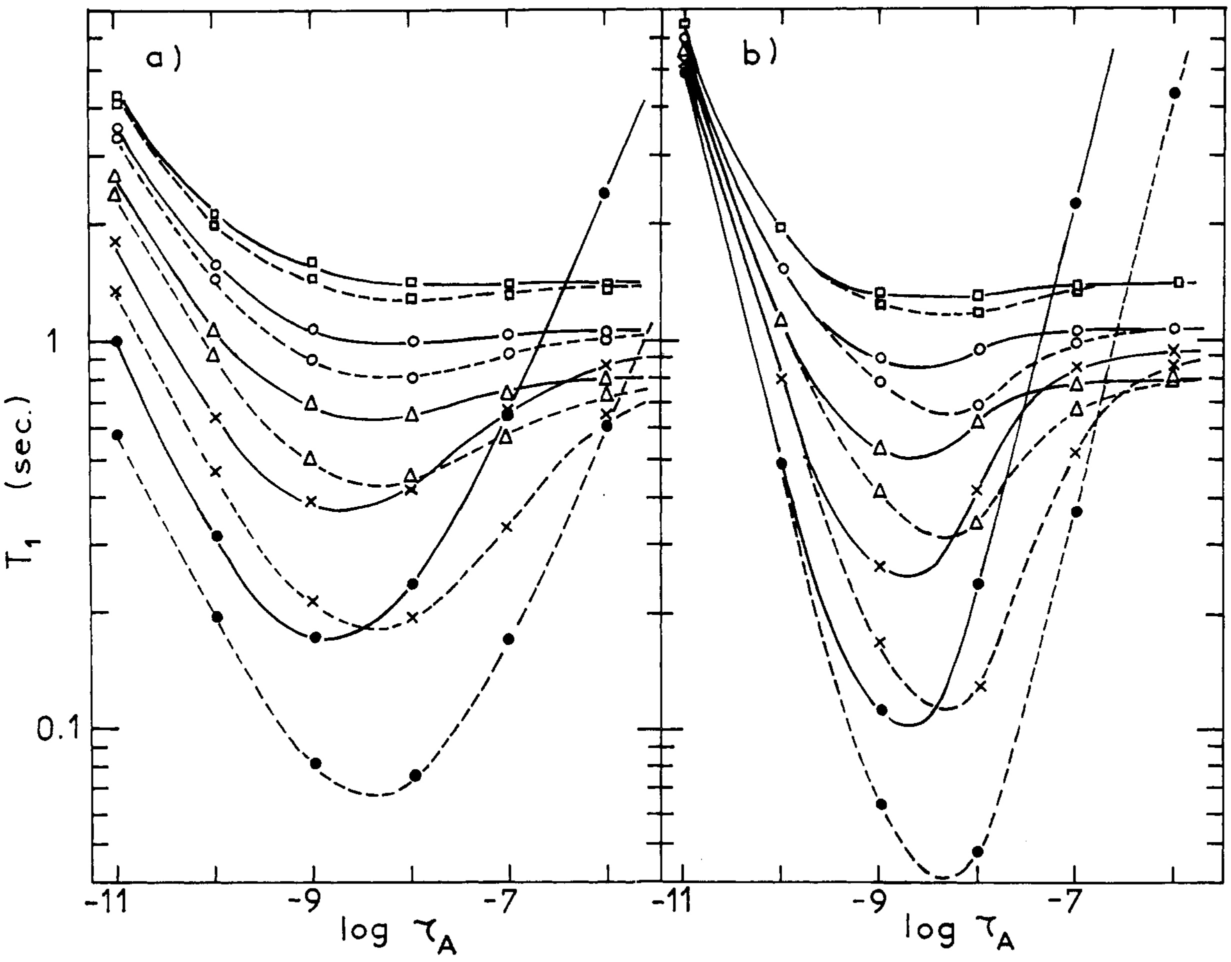

Figure 6. Dependence of T_1 on τ_A for case (1) with $W_1 = 5 \times 10^9$ s^{-1} and W$_2 = 10^{10}$ s^{-1} ($\upsilon = 0.5$). The full and dotted curves are for the resonance frequencies 63 and 25.2 MHz, respectively: (●) C$_0$, (×) C$_1$, (△) C$_2$, (○) C$_3$, (□) C$_4$; (a) $\gamma = 0.6$, and (b) $\gamma = 1$.

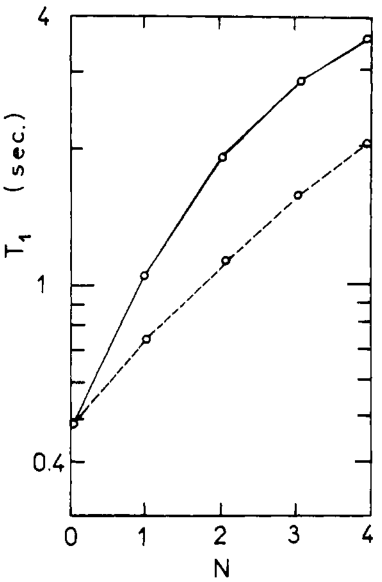

Figure 7. Dependence of T_1 on the carbon number N for case (1) with $W_1 = 5 \times 10^9$ s^{-1} and $W_2 = 10^{10}$ s^{-1} ($v = 0.5$). The full line is for $\gamma = 0.6$ and $\tau_A = 1.6 \times 10^{-11}$ s. The dotted line is for $\gamma = 1$ and $\tau_A = 10^{-10}$ s. The resonance frequency is 25.2 MHz.

Another important piece of information obtained from Figure 6 is that the frequency dependence of T_1 is affected by the distribution. To see this more clearly, T_1 at three different τ_A values is plotted separately against the carbon numbers in Figure 8 together with the NOE. At $\tau_A = 10^{-11}$ and 10^{-7} s, the frequency dependence is larger for $\gamma = 0.6$ than for $\gamma = 1$. On the other hand, at $\tau_A = 5 \times 10^{-9}$ s, near the T_1 minimum, the reverse effect is observed. Although these features may be changed by modifying jump rates, the important point is that we can use such frequency dependences to determine jump rates from experimental data with lesser ambiguity. In other terms, only reliable distribution width and jump rates can account for the data at two frequencies. The ambiguity occurs, at first, in estimating the distribution width. With use of a single frequency, there exist sometimes several possible distribution widths to reproduce the experimental $T_1 \sim 1/T$ curve. This ambiguity can be eliminated by use of two frequencies.[10,16] After obtaining the distribution width, the jump rates for the entire side chain are determined step by step starting from the first carbon up to the end of the side chain varying the jump rates until the calculations are in agreement with the experimental data at two frequencies. Similar procedures have already been applied to the investigation of the molecular motions in poly(L-glutamic acid).[16]

Conclusion and Extension

Although all calculations presented above have been made for particular conditions, they give the essential points of the effects of the distribution of correlation times and the anisotropy of the overall motion on the relaxation of the side chain. In our calculations, we have treated only the saturated hydrocarbon chain, but it is possible to extend the treatment to other types of chains, for example, those containing double bonds, phenyl groups or peptide groups by adjusting the angles ϵ_N, Ω_N, and α_N. If necessary, a combination of different models of the internal rotation may be constructed by replacing the expressions for the ensemble averages (eq 14). For example, if the first bond undergoes unrestricted diffusional rotation, the corresponding expression is $\delta_{aa'} \exp\{-D_1 a^2 \tau\}$,[18] where D_1 is the diffusion coefficient about the first bond. However, in actual cases, a suitable combination may be selected in the procedures of obtaining a satisfactory fitting of the calculations to experimental data at two resonance frequencies. This latter treatment has been applied to poly(alkylvinylpyridines). Our treatments can also be applied to the relaxations due to the quadrupole interaction and the anisotropy of the chemical shift for nuclei having an axially symmetric electric field gradient or chemical shift tensor, respectively, by changing the expressions for the relaxation times.[30]

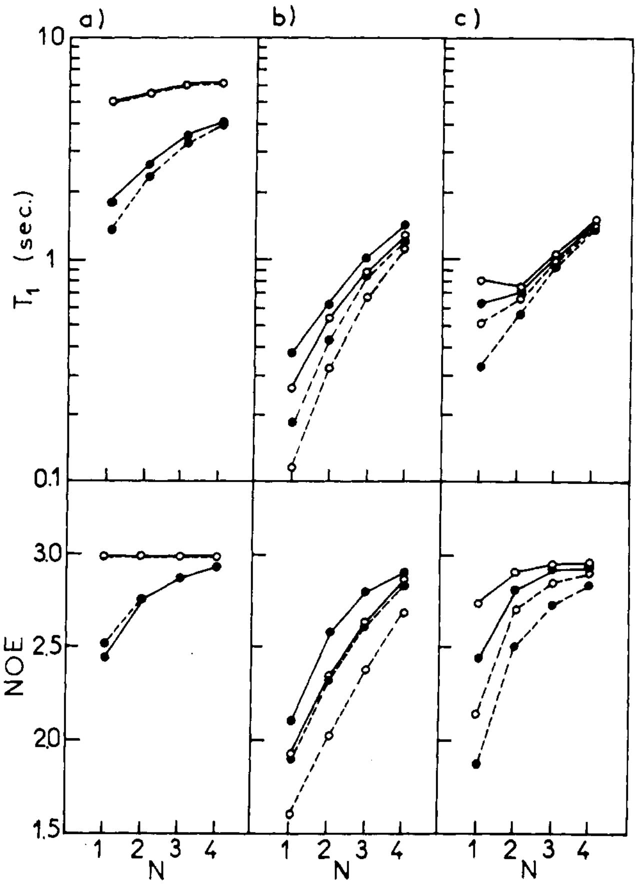

Figure 8. Plot of T_1 and NOE against carbon number N for case (1) with $W_1 = 5 \times 10^9$ s^{-1} and $W_2 = 10^{10}$ s^{-1} ($v = 0.5$). The full and dotted lines correspond to the resonance frequencies 63 and 25.2 MHz, respectively: (○) $\gamma = 1$, (●) $\gamma = 0.6$; (a) $\tau_A = 10^{-11}$ s, (b) $\tau_A = 5 \times 10^{-9}$ s, (c) $\tau_A = 10^{-7}$ s.

For the quadrupole relaxation:

$$T_1^{-1} = 3K_Q\{J_1(\omega) + 4J_2(2\omega)\}$$

$$T^{-1} = \tfrac{1}{2}K_Q\{9J_0(0) + 15J_1(\omega) + 6J_2(2\omega)\}$$

with $K_Q = [e^2qQ/4I\hbar(2I-1)]^2$, and for the chemical shift anisotropy

$$T_1^{-1} = K_c J_1(\omega)$$

$$T_2^{-1} = \tfrac{1}{6}K_c\{4J_0(0) + 3J_1(\omega)\}$$

with $K_c = \{\gamma H_0(\delta_{\parallel} - \delta_{\perp})\}^2$. $(e^2qQ/\hbar)$ is the quadrupole coupling constant and $\delta_{\parallel}$ and $\delta_{\perp}$ are the components of the chemical shift tensor, $\delta_{\parallel}$ refering to the symmetry axis.

Acknowledgment. The authors express their gratitude to Dr. R. Chûjô of Tokyo Institute of Technology and Dr. K. Akasaka of Kyoto University for their valuable advice and discussions.

References and Notes

(1) R. L. Somorjai and R. Deslauriers, *J. Am. Chem. Soc.*, **98**, 6460 (1976).

(2) Y. K. Levine, P. Partington, G. C. K. Roberts, N. J. M. Birdsall, A. G. Lee, and J. C. Metcalfe, *FEBS Lett.*, **22**, 203 (1972).
(3) Y. K. Levine, N. J. M. Birdsall, A. G. Lee, and J. C. Metcalfe, *Biochemistry*, **11**, 1416 (1972).
(4) G. C. Levy, D. E. Axelson, R. Schwartz, and J. Hochman, *J. Am. Chem. Soc.*, **100**, 410 (1978).
(5) R. E. London and J. Avitabile, *J. Am. Chem. Soc.*, **99**, 7765 (1977).
(6) Y. K. Levine, P. Partington, and G. C. K. Roberts, *Mol. Phys.*, **25**, 497 (1973).
(7) F. Heatley, *Polymer*, **16**, 493 (1975).
(8) F. Heatley and A. Begum, *Polymer*, **17**, 399 (1976).
(9) Y. Inoue and T. Konno, *Polym. J.*, **8**, 457 (1976).
(10) D. Ghesquiere, Buu Ban, and C. Chachaty, *Macromolecules*, **10**, 743 (1977).
(11) R. E. London and J. Avitabile, *J. Chem. Phys.*, **65**, 2443 (1976).
(12) Y. K. Levine, *J. Magn. Reson.*, **11**, 421 (1973).
(13) T. Yasukawa and C. Chachaty, *Chem. Phys. Lett.*, **43**, 565 (1976).
(14) T. Yasukawa, D. Ghesquiere, and C. Chachaty, *Chem. Phys. Lett.*, **45**, 279 (1977).
(15) T. Yasukawa and C. Chachaty, *Chem. Phys. Lett.*, **51**, 311 (1977).
(16) A. Tsutsumi, B. Perly, A. Forchioni, and C. Chachaty, *Macromolecules*, **11**, 977 (1978).
(17) D. E. Woessner, *J. Chem. Phys.*, **36**, 1 (1962).
(18) D. Wallach, *J. Chem. Phys.*, **47**, 5258 (1967).
(19) W. T. Huntress, Jr., *Adv. Magn. Reson.*, **14**, 1 (1970).
(20) A. Tsutsumi, *Mol. Phys.*, **37**, 111 (1979).
(21) W. Gronski and N. Murayama, *Makromol. Chem.*, **197**, 1521 (1978).
(22) Y. K. Levine, N. J. M. Birdsall, A. G. Lee, J. C. Metcalfe, P. Partington, and G. C. K. Roberts, *J. Chem. Phys.*, **60**, 2890 (1974).
(23) R. J. Wittebort and A. Szabo, *J. Chem. Phys.*, **69**, 1722 (1978).
(24) Y. K. Levine, *J. Magn. Reson.*, **11**, 421 (1973).
(25) A. A. Jones, *J. Polym. Sci., Polym. Phys. Ed.*, **15**, 863 (1977).
(26) D. Doddrell, V. Glushko, and A. Allerhand, *J. Chem. Phys.*, **56**, 3683 (1972).
(27) D. M. Brink and G. R. Satchler, "Angular Momentum", 2nd ed., Clarendon Press, Oxford, England, 1968.
(28) K. S. Cole and R. H. Cole, *J. Chem. Phys.*, **9**, 341 (1941).
(29) T. M. Connor, *Trans. Faraday Soc.*, **60**, 1574 (1964).
(30) B. D. N. Rao, *Adv. Magn. Reson.*, **4** (1971).

Polymeric Ligands. 9. Oxidation–Reduction Properties of Some Polymeric Thiosemicarbazides Containing Copper Ions[1]

L. Guy Donaruma,*[2] Shinya Kitoh, Gary Walsworth, Joseph V. Depinto, and James K. Edzwald

Department of Chemistry and Department of Civil and Environmental Engineering, Clarkson College of Technology, Potsdam, New York 13676. *Received October 24, 1978*

ABSTRACT: The syntheses of three new poly(thiosemicarbazides) are reported along with those of the respective copper(I) and copper(II) complexes. Oxidation–reduction reactions of the copper complexes of five polymeric thiosemicarbazides, wherein the Cu(I)–Cu(II) "redox" system was employed to reduce or oxidize various organic substrates, are described. "Redox" properties appeared to be related to the nature of the polymer employed to hold the copper.

Results and Discussion

In 1962, Campbell, Foldi, and Tomic[3] reported the preparation of two poly(thiosemicarbazides) (I, II; see Scheme I) which were highly selective for the preferential complexation of copper(II). A problem in utilizing these materials as ion exchangers was that the only useful elutant was aqueous sodium cyanide which, of course, presented certain handling hazards. In attempting to devise selective ion exchange systems which might lower copper(II) concentrations in brass mill effluents to acceptable proportions, we wished to be able to elute the complexed copper(II) from I and II with dilute mineral acid, if possible. Thus, in preparing III–V we attempted to introduce varying degrees of steric hindrance which might weaken the bonding of copper(II) to the poly(thiosemicarbazides). Structures for the copper(II) complexes of I and II are reported[3] and when models of the copper(II) complexes of III–V were constructed, it appeared that the desired steric interactions had been introduced. These interactions were insufficient to allow significant elution with dilute mineral acids, although some improvement was achieved. We then turned to a search for other elutants. Among the large number tried were warm aqueous solutions of 1,4-benzoquinone and hydroquinone. These proved to be successful elutants for the copper(II) complexes of I–V. However, knowing that hydroquinone can be oxidized somewhat easily, we were concerned lest oxidation to 1,4-benzoquinone might have occurred in which case the complexed copper(II) ion would have been reduced to copper(I) thus changing the identity of the ions collected by exchange. However, we could detect no 1,4-benzoquinone.

Having thought about the possibility of oxidation–reduction reactions occurring, we decided to actually attempt a number of these using IIa. We found that upon contacting benzaldehyde with IIa, very good yields of benzoic acid were obtained (see Table I) and that IIa was converted to IIb. There was no difference between IIb prepared from IIa and IIb prepared directly from II and cuprous salts. IIb could be readily oxidized back to IIa with a number of reagents (see Table II), and again there was no difference in the IIa species regardless of how it was prepared. Thus, copper could be repeatedly oxidized or reduced with various substrates without coming off the ion exchanger except when 1,4-benzoquinone was reduced to hydroquinone using IIb.

In the oxidation of benzaldehyde to benzoic acid, the rate of conversion of aldehyde to acid in a 24-h period increased from 18 to 100% as the mole ratio of aldehyde to copper(II) went from 1:1 to 1:5. Further, we found that the nature of the poly(thiosemicarbazide) used to form Ia–Va profoundly altered the yields of benzoic acid over the same reaction time under identical reaction conditions (see Table III).

It is interesting to note that a special situation exists here in that the copper is so tightly bound to the poly(thiosemicarbazide) that it is possible to carry out oxidation–reduction reactions under extremely simple reaction conditions which give good yields of various products and no loss of copper (save in the quinone–hy-

0024-9297/79/2212-0435$01.00/0